

# Impact of Circular Thickness on Vibrational Frequency of Orthotropic Rectangular Plate

Neeraj Lather<sup>1</sup>, Vijil kumar<sup>2</sup>, Ankit Kumar<sup>3</sup>, Amit Sharma\*<sup>1</sup>, Sapna<sup>1</sup>, and Reeta Bhardwaj<sup>1</sup>

<sup>1</sup>Department of Mathematics, Amity University Haryana, Gurugram, India

<sup>2</sup>School of Applied Sciences (Mathematics), Kalinga Institute of Industrial Technology (KIIT), Bhubaneswar-751024, Odisha, India

<sup>3</sup>Chitkara University School of Engineering & Technology, Chitkara University, Solon, Himachal Pradesh 174103, India

## Abstract

The objective of this study is to investigate the natural vibration of a rectangular plate made of orthotropic material with circular thickness (two dimensions) and temperature variation on the plate is parabolic(two dimensions) in nature. Various plate parameters, including tapering parameters, thermal gradient, and aspect ratio, are taken into account. The solution to the problem is obtained by utilizing the Rayleigh-Ritz technique and the first four frequency modes are obtained under clamped edge conditions. The obtained numerical outcomes are compared with previous literature. Although previous investigations revealed that the effect of two dimension thickness (linear, parabolic) on vibration frequency of orthotropic rectangular plates has been studied but the effect of two dimension circular thickness has not been explored. This study examines the circular thickness variation and finds that it significantly reduces the variation in frequency modes compared to earlier studies done. Furthermore, the time period changes at a slower rate for this particular circular variation in thickness. The results of this research are expected to have practical significance in design applications.

**Keywords:** Orthotropic rectangular plate, thermal gradient, circular tapering, aspect ratio.

## 1 Introduction

To design structures or understand system characteristics, it becomes vital to investigate the vibrational properties of plates. Many systems and structures such as bridges, buildings, and

---

\*Email: dba.amitsharma@gmail.com, Corresponding Author

aircraft wings consist of plates of various shapes. The vibration characteristics of a plate are influenced by plate parameters such as tapering, non-homogeneity (in the case of nonhomogeneous materials), and thermal gradient. A considerable number of studies in the literature have focused on various values of plate parameters.

The approach outlined in [1] was utilized to amalgamate solutions for plates with different geometries (such as circular, annular, circular sector, and annular sector plates) under various boundary conditions. The same method was employed to study the vibration problem of an orthotropic circular plate, which has thickness that exponentially varies in the radial direction and is subjected to a quadratic temperature distribution. Classical plate theory was employed in [2] to study a plate with edge conditions on a Winkler elastic foundation. The study reported in [3] examined the natural vibrations of thin rectangular plates made of isotropic and orthotropic materials, with thickness that is either constant or variable. Both Finite

Element Method and Finite Difference Method were employed to analyze the problem, considering different boundary conditions. In [4], a solution that provides accuracy for the in-plane free vibration analysis of orthotropic rectangular plates under diverse boundary conditions was presented, utilizing the method of reverberation ray matrix (MRRM). In [5], the authors discussed analytical solutions for the free vibration problem of inhomogeneous orthotropic rectangular plates (IHORPs) supported by an inhomogeneous viscoelastic foundation (IHVEF). In [6], a theory of elasticity was developed to analyze the free vibration of embedded orthotropic thick circular and elliptical nano-plates supported by an elastic foundation. In [7], a novel solution that is asymptotically precise was derived for the issue of transverse vibrations in a rectangular orthotropic plate with free edges. In [8], formulations using finite elements were introduced for analyzing the free vibration of isotropic and orthotropic plates based on the two-variable refined plate theory. In [9], a numerical method was used to study the free transverse vibration of an orthotropic thin trapezoidal plate with parabolic thickness in the  $x$ -direction under a linear temperature distribution in the  $x$ -direction. [10] employed exponential shear deformation theory to evaluate the critical buckling loads and natural frequencies of orthotropic plates. In [11], the vibrational behavior of a thin square orthotropic plate placed on a non-uniform elastic foundation was conducted using the element-free Galerkin method. New precise analytical solutions were proposed in [12] to analyze the free vibration behavior of thin orthotropic rectangular plates, while the forced response of polar orthotropic tapered circular plates placed on an elastic foundation was investigated in [13]. In [14], the wave-based method (WBM) was utilized to forecast the flexural vibrations of orthotropic plates. In [15], a solution based on two-variable refined plate theory of Levy type was developed for free vibration analysis of orthotropic plates. In [16], a new analytical solution utilizing a double finite sine integral transform technique was introduced for the vibration response of plates reinforced by orthogonal beams. In [17], the Rayleigh Ritz method was utilized to determine the frequency of an orthotropic rectangular plate, whereas in [18], the time period of transverse vibration of a skew plate with different edge conditions was assessed. In [19], the influence of temperature on the frequencies of a tapered plate was discussed, while [20] investigated a non-uniform triangular plate subjected to a two-dimensional parabolic temperature distribution. The investigation of time period of rectangular plates with varying thickness and temperature was examined in [21]. Time period analysis of isotropic and orthotropic visco skew plate having circular variation in thickness and density at different edge conditions is discussed in [22] and [23].

It is noticeable from the literature that most of the authors have investigated either linear or parabolic variations in tapering parameters, but no one has focused on circular variation in

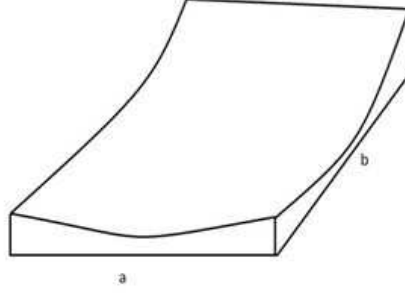


Figure 1: Orthotropic rectangular plate with  $2D$  circular thickness.

tapering parameter. This study aims to fill this research gap by exploring the influence of two dimension circular thickness on the vibrational frequency of an orthotropic rectangular plate under a two dimension parabolic temperature profile. The circular variation examined in this paper results in a reduction in the variation in frequency modes, as shown in the numerical results section. Furthermore, the chosen circular variation reduces the variation in frequency modes, time period as compared to the available published results, which are presented in the comparative analysis.

## 2 Problem geometry and analysis

Taking into account that the nonhomogeneous rectangular plate shown in Figure (1) with sides  $a$ ,  $b$  and thickness  $l$ .

The formulation of the kinetic energy and strain energy for plate vibration is given below, similar to the approach presented in [24]

$$T_s = \frac{1}{2}\omega^2 \int_0^a \int_0^b l\Phi^2 d\psi d\zeta \quad (1)$$

$$V_s = \frac{1}{2} \int_0^a \int_0^b \left[ D_\zeta \left( \frac{\partial^2 \Phi}{\partial \zeta^2} \right)^2 + D_\psi \left( \frac{\partial^2 \Phi}{\partial \psi^2} \right)^2 + 2\nu_\zeta D_\psi \frac{\partial^2 \Phi}{\partial \zeta^2} \frac{\partial^2 \Phi}{\partial \psi^2} + 4D_{\zeta\psi} \left( \frac{\partial^2 \Phi}{\partial \zeta \partial \psi} \right)^2 \right] d\psi d\zeta \quad (2)$$

where  $\phi$  is deflection function,  $\omega$  is natural frequency,  $D_\zeta = E_\zeta l^3/12(1 - \nu_\zeta \nu_\psi)$ ,  $D_\psi = E_\psi l^3/12(1 - \nu_\zeta \nu_\psi)$ ,  $D_{\zeta\psi} = E_\zeta l^3/12(1 - \nu_\zeta \nu_\psi)$ . Here,  $D_\zeta$  and  $D_\psi$  is flexural rigidity in  $\zeta$  and  $\psi$  directions respectively and  $D_{\zeta\psi}$  is torsional rigidity.

In order to address the investigated problem, the Rayleigh-Ritz method is utilized, which necessitates

$$L = \delta(V_s - T_s) = 0. \quad (3)$$

Using Eqs. (1), (2), we have

$$L = \frac{1}{2} \int_0^a \int_0^b \left[ D_\zeta \left( \frac{\partial^2 \Phi}{\partial \zeta^2} \right)^2 + D_\psi \left( \frac{\partial^2 \Phi}{\partial \psi^2} \right)^2 + 2\nu_\zeta D_\psi \frac{\partial^2 \Phi}{\partial \zeta^2} \frac{\partial^2 \Phi}{\partial \psi^2} + 4D_{\zeta\psi} \left( \frac{\partial^2 \Phi}{\partial \zeta \partial \psi} \right)^2 \right] d\psi d\zeta - \frac{1}{2} \omega^2 \int_0^a \int_0^b \Phi^2 d\psi d\zeta = 0. \quad (4)$$

Proposing non-dimensional variable as

$$\zeta_1 = \zeta/a, \quad \psi_1 = \psi/a$$

along with two dimension circular thickness as

$$l = l_0 \left( 1 + \beta_1 \left\{ 1 - \sqrt{1 - \zeta_1^2} \right\} \right) \left( 1 + \beta_2 \left\{ 1 - \sqrt{1 - \frac{a^2}{b^2} \psi_1^2} \right\} \right) \quad (5)$$

where  $l_0$  is thickness at origin and  $\beta_1, \beta_2 \leq 1$  are tapering parameters.

The two-dimensional parabolic temperature distribution, as presented in Eq (6)

$$\tau = \tau_0 (1 - \zeta_1^2) \left( 1 - \frac{a^2 \psi_1^2}{b^2} \right), \quad (6)$$

Here  $\tau$  and  $\tau_0$  represent the temperature at a given point and at the origin respectively.

For orthotropic materials, modulus of elasticity is by For orthotropic materials, modulus of elasticity is evaluated by

$$E_\zeta = E_1 (1 - \gamma\tau), \quad E_\psi = E_2 (1 - \gamma\tau), \quad G_{\zeta\psi} = G_0 (1 - \gamma\tau), \quad (7)$$

where  $E_\zeta$  and  $E_\psi$  are the Young's modulus in  $\zeta$  and  $\psi$  directions,  $G_{\zeta\psi}$  is shear modulus and  $\gamma$  is called slope of variation. Using Eq. (6), Eq. (7) becomes

$$\begin{aligned} E_\zeta &= E_1 \left( 1 - \alpha (1 - \zeta_1^2) \left( 1 - \frac{a^2 \psi_1^2}{b^2} \right) \right), \\ E_\psi &= E_2 \left( 1 - \alpha (1 - \zeta_1^2) \left( 1 - \frac{a^2 \psi_1^2}{b^2} \right) \right), \\ G_{\zeta\psi} &= G_0 \left( 1 - \alpha (1 - \zeta_1^2) \left( 1 - \frac{a^2 \psi_1^2}{b^2} \right) \right), \end{aligned} \quad (8)$$

where  $\alpha = \gamma\tau_0$  ( $0 \leq \alpha < 1$ ) is called thermal gradient. Using Eqs. (5), (8) and non dimensional variable, the functional in Eq. (4) become

$$\begin{aligned}
L = \frac{D_0}{2} \int_0^1 \int_0^{\frac{b}{a}} & \left[ \left( 1 - \alpha (1 - \zeta_1^2) \left( 1 - \frac{a^2 \psi_1^2}{b^2} \right) \right) \left( 1 + \beta_1 \left\{ 1 - \sqrt{1 - \zeta_1^2} \right\} \right)^3 \right. \\
& \left. \left( 1 + \beta_2 \left\{ 1 - \sqrt{1 - \frac{a^2}{b^2} \psi_1^2} \right\} \right)^3 \left\{ \left( \frac{\partial^2 \Phi}{\partial \zeta_1^2} \right)^2 + \frac{E_2}{E_1} \left( \frac{\partial^2 \Phi}{\partial \psi_1^2} \right)^2 \right. \right. \\
& \left. \left. + 2\nu_\zeta \frac{E_2}{E_1} \left( \frac{\partial^2 \Phi}{\partial \zeta_1^2} \right) \left( \frac{\partial^2 \Phi}{\partial \psi_1^2} \right) + 4 \frac{G_0}{E_1} (1 - \nu_\zeta \nu_\psi) \left( \frac{\partial^2 \Phi}{\partial \zeta_1 \partial \psi_1} \right)^2 \right\} \right] \\
& d\psi_1 d\zeta_1 - \lambda^2 \int_0^1 \int_0^{\frac{b}{a}} \left[ \left( 1 + \beta_1 \left\{ 1 - \sqrt{1 - \zeta_1^2} \right\} \right) \right. \\
& \left. \left( 1 + \beta_2 \left\{ 1 - \sqrt{1 - \frac{a^2}{b^2} \psi_1^2} \right\} \right) \right] \Phi^2 d\psi_1 d\zeta_1 = 0 \tag{9}
\end{aligned}$$

where

$$D_0 = \frac{1}{2} \left( \frac{E_1 l_0^3}{12 (1 - \nu_\zeta \nu_\psi)} \right) \text{ and } \lambda^2 = \frac{12 a^4 \rho \omega^2 (1 - \nu_\zeta \nu_\psi)}{E_1 h_0^2}$$

The deflection function that meets all the edge conditions is taken as in [25]

$$\begin{aligned}
\Phi(\zeta, \psi) = & \left[ (\zeta_1)^e (\psi_1)^f (1 - \zeta_1)^g \left( 1 - \frac{a\psi_1}{b} \right)^h \right] \\
& \left[ \sum_{i=0}^n \Psi_i \left\{ (\zeta_1) (\psi_1) (1 - \zeta_1) \left( 1 - \frac{a\psi_1}{b} \right) \right\}^i \right] \tag{10}
\end{aligned}$$

where  $\Psi_i, i = 0, 1, 2, \dots, n$  are unknowns and the value of e, f, g, h can be 0, 1 and 2, corresponding to given edge condition. Eq. (10) can be minimized by imposing the following condition.

$$\frac{\partial L}{\partial \Psi_i} = 0, \quad i = 0, 1, \dots, n. \tag{11}$$

Solving Eq. (11), we have frequency equation

$$|P - \lambda^2 Q| = 0 \tag{12}$$

where  $P = [p_{ij}]_{i,j=0,1,\dots,n}$  and  $Q = [q_{ij}]_{i,j=0,1,\dots,n}$  are square matrix of order  $(n + 1)$ .

### 3 Numerical results and discussions

In this study, the first four natural frequencies of a clamped orthotropic rectangular plate with two dimension circular thickness and two dimension parabolic temperature variations are investigated corresponding to various plate parameters aspect ratio  $\frac{a}{b}$ , tapering parameters  $\beta_1$  and  $\beta_2$ , and thermal gradient  $\alpha$ . The frequency equation of the plate is solved using the Rayleigh-Ritz technique, and the results are presented in tabular form for ease of interpretation. The

numerical calculations are based on the subsequent parameter values:

$$E = 0.04, E_1 = 1, E_2 = 0.32, G = 0.09, \rho = 2.80103 \text{ kg}/M^3, \text{ and } \nu = 0.345.$$

Table 1 presents the natural frequencies (first four modes) of a clamped orthotropic rectangular plate with a fixed value of tapering parameter  $\beta_2$  and thermal gradient  $\alpha$ , but different values of tapering parameter  $\beta_1$ . Specifically, the values of  $\beta_2 = \alpha$  chosen were 0.2, 0.4, and 0.6 respectively. Based on the results presented in Table 1, it can be inferred that:

- (i) The frequency modes increase in all four modes as the tapering parameter  $\beta_1$  rises from 0.0 to 1.0.
- (ii) As both the tapering parameter  $\beta_1$  and thermal gradient  $\alpha$  increase from 0.2 to 0.6 (i.e.,  $\beta_2 = \alpha = 0.2$  to  $\beta_2 = \alpha = 0.6$ ), the modes of frequency also show an increment.
- (iii) The modes of frequency (rate of increment) are predominantly influenced by the tapering parameter  $\beta_1$ , as opposed to the thermal gradient  $\alpha$  and tapering parameter  $\beta_2$ .

Table 2 presents the modes of frequency (first four modes) of a clamped orthotropic rectangular plate corresponding to the tapering parameter  $\beta_2$ , with fixed values of tapering parameter  $\beta_1$  and thermal gradient  $\alpha$  i.e.,  $\beta_1 = \alpha = 0.2$ ,  $\beta_1 = \alpha = 0.4$ , and  $\beta_1 = \alpha = 0.6$ , respectively. Based on the findings in Table 2, it is evident that:

- (i) The modes of frequency exhibit an increase as the tapering parameter  $\beta_2$  varies from 0.0 to 1.0.
- (ii) The modes of frequency decrease as the tapering parameter  $\beta_1$  and thermal gradient  $\alpha$  increase from 0.2 to 0.6 (i.e.,  $\beta_1 = \alpha = 0.2$  to  $\beta_1 = \alpha = 0.6$ ), when the tapering parameter  $\beta_2$  changes from 0.0 to 0.6. However, the modes of frequency increase as the tapering parameter  $\beta_1$  and thermal gradient  $\alpha$  increase from 0.2 to 0.6 (i.e.,  $\beta_1 = \alpha = 0.2$  to  $\beta_1 = \alpha = 0.6$ ), when the tapering parameter  $\beta_2$  varies from 0.8 to 1.0.
- (iii) In terms of the rate of change in modes of frequency, the tapering parameter  $\beta_2$  exerts a stronger influence compared to the thermal gradient  $\alpha$  and the tapering parameter  $\beta_1$ .
- (iv) The tables 1 and 2 indicate that the modes of frequency are primarily influenced by the tapering parameter  $\beta_2$  as compared to the tapering parameter  $\beta_1$ .

Table 3 presents the modes of frequency (first four modes) of a clamped orthotropic rectangular plate for various values of thermal gradient  $\alpha$ , while keeping both tapering parameters  $\beta_1$  and  $\beta_2$  fixed at 0.2, 0.4, and 0.6, respectively. By examining Table 3, the subsequent key findings can be observed:

- (i) The frequency modes also increase with an increase in tapering parameters  $\beta_1$  and  $\beta_2$  from 0.0 to 1.0, while the modes of frequency decrease with an increase in the value of thermal gradient  $\alpha$  from 0.0 to 1.0.
- (ii) Compared to the tapering parameters  $\beta_1$  and  $\beta_2$ , the thermal gradient  $\alpha$  has a greater influence on the modes of frequency (i.e., rate of change in the modes of frequency).

Table 4 presents the first four modes of frequency of a clamped orthotropic rectangular plate for fixed values of the tapering parameters  $\beta_1, \beta_2$ , and thermal gradient  $\alpha$ , corresponding to the aspect ratio  $a/b$ . The fixed values of  $\beta_1, \beta_2$ , and  $\alpha$  are 0.2, 0.4, and 0.6, respectively. In this table, the authors investigate the effect of varying the aspect ratio in the range of 0.25 to 1.50. Based on Table 4, it is observed that:

- (i) The modes of frequency exhibit a sharp decline for aspect ratios between 0.25 to 0.5, whereas the drop is less abrupt and the rate of decline becomes slower for aspect ratios greater than 0.5.
- (ii) Another interesting observation is that the modes of frequency increase as the other parameters, including the tapering parameters  $\beta_1, \beta_2$ , and thermal gradient  $\alpha$ , increase.
- (iii) It is worth noting that for an aspect ratio of  $\frac{a}{b} = 0.25$ , the modes of frequency are much higher than those for aspect ratios ranging from  $\frac{a}{b} = 0.5$  to 1.5. This suggests that a smaller aspect ratio leads to higher modes of frequency, and vice versa.

## 4 Convergence study

In this section, a study is conducted to investigate the convergence of the frequency modes for an orthotropic rectangular plate at clamped edge conditions. The study involves increasing the order of approximation for all plate parameters within the specified ranges, i.e.,  $E = 0.04$ ,  $E_1 = 1$ ,  $E_2 = 0.32$ ,  $G = 0.09$ ,  $\beta_1 = \beta_2 = m = \alpha = 0$ . The outcomes of this study are presented in Table 5 for analysis. The table demonstrates that the frequency modes of the orthotropic rectangular plate converge up to four decimal places in the fifth approximation.

## 5 Comparison of results

In this section, the authors provide a comparative analysis between the time period  $K$  obtained in their study and the previously published results. Tables 6 and 7 provide a comparative analysis of the time period of a clamped orthotropic rectangular plate (present study) with the time period obtained in [26] and [27], for fixed values of thermal gradient  $\alpha = 0.3$  and aspect ratio 1.5 corresponding to both tapering parameters  $\beta_1$  and  $\beta_2$ . The comparison shows that the time period obtained in the present study is higher than that obtained in [26] and [27]. However, the decrement rate in the time period obtained in the present study is much less than that obtained in [26] and [27]. Additionally, the tables reveal that the time period obtained in the present study and the time period obtained in [26] and [27] coincide initially at  $\beta_1 = \beta_2 = 0.0$ .

## 6 Conclusions

Based on the numerical findings and comparative analysis, the present study examines the first four modes of vibration of a clamped orthotropic rectangular plate for three plate parameters: tapering  $\beta_1, \beta_2$ , thermal gradient  $\alpha$ , and aspect ratio  $a/b$ . The following observations can be made:

- (i) The current study revealed that circular tapering results in a higher time period compared to linear tapering (refer Table 6)
- (ii) The time period obtained for circular tapering in the present study is higher compared to the time period obtained for parabolic tapering (refer Table 7).
- (iii) The rate of decrement in the time period obtained from circular tapering in the present study is much lower compared to the time period obtained from parabolic tapering and linear tapering (refer Tables 6 and 7).
- (iv) The increase in tapering parameters  $\beta_1$  and  $\beta_2$  leads to an increase in frequency modes, while an increase in thermal gradient  $\alpha$  and aspect ratio  $a/b$  causes a decrease in frequency modes.
- (v) A sudden drop in frequency modes is observed when the aspect ratio  $a/b$  is increased from 0.25 to 0.5.
- (vi) Higher modes of frequency are observed when the aspect ratio is smaller and vice versa.

The above observation suggests that the plate parameters have a significant impact on the frequency modes of the plate. The selection of appropriate plate parameters can enable the manipulation of frequency modes, time period, and their variations as per the system requirements. Thus, it can be inferred that circular variation in plate parameters can be effective in minimizing and regulating frequency modes, time period, and their variations.

Table 1: Modes of frequency of clamped orthotropic rectangular plate corresponding to tapering parameter  $\beta_1$ .

$\beta_1$	$\alpha = \beta_2 = 0.2$				$\alpha = \beta_2 = 0.4$				$\alpha = \beta_2 = 0.6$			
	$\lambda_1$	$\lambda_2$	$\lambda_3$	$\lambda_4$	$\lambda_1$	$\lambda_2$	$\lambda_3$	$\lambda_4$	$\lambda_1$	$\lambda_2$	$\lambda_3$	$\lambda_4$
0.0	17.002	65.265	146.471	335.761	17.085	64.734	145.409	344.526	17.173	64.058	144.568	353.913
0.2	17.747	67.704	151.913	351.645	17.848	67.198	151.149	359.343	17.951	66.545	150.178	372.482
0.4	18.548	70.301	157.829	367.708	18.665	69.815	156.993	378.568	18.782	69.169	156.353	390.070
0.6	19.400	73.032	163.844	388.066	19.531	72.556	163.396	397.071	19.660	71.918	162.620	412.912
0.8	20.295	75.877	170.500	405.951	20.439	75.414	169.982	417.520	20.579	74.769	169.561	432.019
1.0	21.228	78.822	177.057	430.024	21.385	78.367	176.579	443.749	21.534	77.713	176.455	457.574

Table 2: Modes of frequency of clamped orthotropic rectangular plate corresponding to tapering parameter  $\beta_2$ .

$\beta_2$	$\alpha = \beta_1 = 0.2$				$\alpha = \beta_1 = 0.4$				$\alpha = \beta_1 = 0.6$			
	$\lambda_1$	$\lambda_2$	$\lambda_3$	$\lambda_4$	$\lambda_1$	$\lambda_2$	$\lambda_3$	$\lambda_4$	$\lambda_1$	$\lambda_2$	$\lambda_3$	$\lambda_4$
0.0	16.884	64.897	145.678	331.631	16.821	63.931	143.466	335.190	16.745	62.771	141.247	338.296
0.2	17.747	67.706	151.891	351.687	17.708	66.777	150.105	354.357	17.653	65.651	147.834	361.409
0.4	18.682	70.704	158.882	372.279	18.665	69.811	157.040	378.477	18.628	68.707	155.163	384.197
0.6	19.679	73.876	165.970	397.993	19.682	73.008	164.524	402.674	19.660	71.922	162.578	413.001
0.8	20.728	77.179	173.823	421.552	20.748	76.333	172.421	428.978	20.740	75.245	170.879	438.255
1.0	21.820	80.596	181.651	451.845	21.855	79.765	180.352	461.690	21.860	78.678	179.140	470.506



Table 3: Modes of frequency of clamped orthotropic rectangular plate corresponding to thermal gradient  $\alpha$ .

$\alpha$	$\beta_1 = \beta_2 = 0.2$				$\beta_1 = \beta_2 = 0.4$				$\beta_1 = \beta_2 = 0.6$			
	$\lambda_1$	$\lambda_2$	$\lambda_3$	$\lambda_4$	$\lambda_1$	$\lambda_2$	$\lambda_3$	$\lambda_4$	$\lambda_1$	$\lambda_2$	$\lambda_3$	$\lambda_4$
0.0	18.539	70.998	159.217	364.788	20.306	76.727	172.199	403.590	22.244	82.942	186.104	449.270
0.2	17.747	67.705	151.912	351.645	19.507	73.367	164.790	391.249	21.429	79.480	178.659	437.433
0.4	16.912	64.226	144.209	338.017	18.665	69.816	156.984	378.585	20.571	75.821	170.826	425.369
0.6	16.027	60.520	136.028	323.885	17.772	66.023	148.867	365.262	19.660	71.917	162.636	412.879
0.8	15.079	56.527	127.337	309.053	16.816	61.942	140.183	351.597	18.684	67.710	153.955	400.094
1.0	14.050	52.161	118.026	293.397	15.777	57.482	130.883	337.433	17.620	63.109	144.730	386.914

Table 4: Modes of frequency of clamped orthotropic rectangular plate corresponding to aspect ratio  $\frac{a}{b}$

$\frac{a}{b}$	$\alpha = \beta_1 = \beta_2 = 0.2$				$\alpha = \beta_1 = \beta_2 = 0.4$				$\alpha = \beta_1 = \beta_2 = 0.6$			
	$\lambda_1$	$\lambda_2$	$\lambda_3$	$\lambda_4$	$\lambda_1$	$\lambda_2$	$\lambda_3$	$\lambda_4$	$\lambda_1$	$\lambda_2$	$\lambda_3$	$\lambda_4$
0.25	376.134	1450.000	3270.490	7745.400	395.177	1494.260	3386.920	8283.150	415.741	1538.250	3508.830	9076.100
0.5	96.028	369.228	832.078	1956.370	100.916	380.582	860.581	2100.440	106.199	391.840	891.569	2300.390
0.75	45.083	172.736	388.186	910.777	47.395	178.078	401.497	977.430	49.897	183.394	416.243	1061.990
1.0	28.176	107.627	241.596	560.835	29.630	110.969	249.643	605.142	31.206	114.308	258.632	659.019
1.25	21.094	80.453	180.911	413.387	22.186	82.966	186.506	450.033	23.370	85.465	193.203	490.725
1.5	17.747	67.705	151.912	351.645	18.665	69.816	156.984	378.585	19.660	71.917	162.636	412.879

Table 5: Convergence study of modes of frequency of orthotropic rectangle plate

$N$	$\lambda_1$	$\lambda_2$
2	16.9543	68.1543
3	16.9543	65.7956
4	16.9543	65.7620
5	16.9543	65.7620

Table 6: Comparison of time period of present study (orthotropic rectangular plate) and obtained in ([26]) corresponding to both tapering parameters  $\beta_1, \beta_2$  for fixed value of aspect ratio  $\frac{a}{b} = 1.5$

$\beta_1$		$\alpha = 0.3$											
		$\beta_2 = 0.0$		$\beta_2 = 0.2$		$\beta_2 = 0.4$		$\beta_2 = 0.6$		$\beta_2 = 0.8$		$\beta_2 = 1.0$	
		$K_1$	$K_2$	$K_1$	$K_2$	$K_1$	$K_2$	$K_1$	$K_2$	$K_1$	$K_2$	$K_1$	$K_2$
0.0	0.09916	0.39898	0.09410	0.37869	0.08906	0.35890	0.08416	0.34002	0.07947	0.32223	0.07503	0.30560	
	<b>0.09916</b>	<b>0.39898</b>	<b>0.08922</b>	<b>0.35924</b>	<b>0.08057</b>	<b>0.32478</b>	<b>0.07313</b>	<b>0.29522</b>	<b>0.06674</b>	<b>0.26990</b>	<b>0.06125</b>	<b>0.24816</b>	
0.2	0.09493	0.38145	0.09014	0.36245	0.08538	0.34388	0.08074	0.32610	0.07629	0.30931	0.07208	0.29357	
	<b>0.08950</b>	<b>0.36015</b>	<b>0.08055</b>	<b>0.32437</b>	<b>0.07275</b>	<b>0.29335</b>	<b>0.06604</b>	<b>0.26672</b>	<b>0.06029</b>	<b>0.24390</b>	<b>0.05534</b>	<b>0.22430</b>	
0.4	0.09071	0.36427	0.08620	0.34649	0.08171	0.32908	0.07732	0.31239	0.07312	0.29657	0.06914	0.28172	
	<b>0.08117</b>	<b>0.32676</b>	<b>0.07307</b>	<b>0.29438</b>	<b>0.06601</b>	<b>0.26631</b>	<b>0.05994</b>	<b>0.24221</b>	<b>0.05473</b>	<b>0.22156</b>	<b>0.05025</b>	<b>0.20380</b>	
0.6	0.08656	0.34762	0.08232	0.33100	0.07809	0.31473	0.07396	0.29906	0.07000	0.28419	0.06623	0.27018	
	<b>0.07402</b>	<b>0.29813</b>	<b>0.06665</b>	<b>0.26868</b>	<b>0.06023</b>	<b>0.24313</b>	<b>0.05470</b>	<b>0.22120</b>	<b>0.04996</b>	<b>0.20240</b>	<b>0.04588</b>	<b>0.18623</b>	
0.8	0.08253	0.33169	0.07855	0.31617	0.07457	0.30092	0.07069	0.28623	0.06695	0.27225	0.06340	0.25905	
	<b>0.06788</b>	<b>0.27357</b>	<b>0.06113</b>	<b>0.24660</b>	<b>0.05526</b>	<b>0.22322</b>	<b>0.05020</b>	<b>0.20315</b>	<b>0.04585</b>	<b>0.18593</b>	<b>0.04211</b>	<b>0.17112</b>	
1.0	0.07867	0.31658	0.07492	0.30205	0.07119	0.28777	0.06754	0.27399	0.06402	0.26083	0.06067	0.24839	
	<b>0.06258</b>	<b>0.25238</b>	<b>0.05637</b>	<b>0.22755</b>	<b>0.05096</b>	<b>0.20604</b>	<b>0.04631</b>	<b>0.18756</b>	<b>0.04231</b>	<b>0.17171</b>	<b>0.03886</b>	<b>0.15807</b>	

Bold values are obtained from [26]

Table 7: Comparison of time period of present study (orthotropic rectangular plate) and obtained in ([27]) corresponding to both tapering parameters  $\beta_1, \beta_2$  for fixed value of aspect ratio  $\frac{a}{b} = 1.5$

$\beta_1$		$\alpha = 0.3$											
		$\beta_2 = 0.0$		$\beta_2 = 0.2$		$\beta_2 = 0.4$		$\beta_2 = 0.6$		$\beta_2 = 0.8$		$\beta_2 = 1.0$	
		$K_1$	$K_2$	$K_1$	$K_2$	$K_1$	$K_2$	$K_1$	$K_2$	$K_1$	$K_2$	$K_1$	$K_2$
0.0	0.09916	0.39898	0.09410	0.37869	0.08906	0.35890	0.08416	0.34002	0.07947	0.32223	0.07503	0.30560	
	<b>0.09916</b>	<b>0.39898</b>	<b>0.09143</b>	<b>0.36804</b>	<b>0.08407</b>	<b>0.33910</b>	<b>0.07727</b>	<b>0.31274</b>	<b>0.07112</b>	<b>0.28912</b>	<b>0.06561</b>	<b>0.26808</b>	
0.2	0.09493	0.38145	0.09014	0.36245	0.08538	0.34388	0.08074	0.32610	0.07629	0.30931	0.07208	0.29357	
	<b>0.09241</b>	<b>0.37124</b>	<b>0.08530</b>	<b>0.34297</b>	<b>0.07851</b>	<b>0.31645</b>	<b>0.07224</b>	<b>0.29225</b>	<b>0.06655</b>	<b>0.27048</b>	<b>0.06145</b>	<b>0.25103</b>	
0.4	0.09071	0.36427	0.08620	0.34649	0.08171	0.32908	0.07732	0.31239	0.07312	0.29657	0.06914	0.28172	
	<b>0.08595</b>	<b>0.34507</b>	<b>0.07942</b>	<b>0.31931</b>	<b>0.07319</b>	<b>0.29507</b>	<b>0.06741</b>	<b>0.27287</b>	<b>0.06217</b>	<b>0.25283</b>	<b>0.05746</b>	<b>0.23490</b>	
0.6	0.08656	0.34762	0.08232	0.33100	0.07809	0.31473	0.07396	0.29906	0.07000	0.28419	0.06623	0.27018	
	<b>0.07991</b>	<b>0.32095</b>	<b>0.07392</b>	<b>0.29741</b>	<b>0.06820</b>	<b>0.27523</b>	<b>0.06289</b>	<b>0.25486</b>	<b>0.05806</b>	<b>0.23643</b>	<b>0.05371</b>	<b>0.21987</b>	
0.8	0.08253	0.33169	0.07855	0.31617	0.07457	0.30092	0.07069	0.28623	0.06695	0.27225	0.06340	0.25905	
	<b>0.07435</b>	<b>0.29896</b>	<b>0.06885</b>	<b>0.27741</b>	<b>0.06359</b>	<b>0.25706</b>	<b>0.05871</b>	<b>0.23834</b>	<b>0.05425</b>	<b>0.22134</b>	<b>0.05024</b>	<b>0.20605</b>	
1.0	0.07867	0.31658	0.07492	0.30205	0.07119	0.28777	0.06754	0.27399	0.06402	0.26083	0.06067	0.24839	
	<b>0.06929</b>	<b>0.27909</b>	<b>0.06423</b>	<b>0.25928</b>	<b>0.05939</b>	<b>0.24056</b>	<b>0.05488</b>	<b>0.22329</b>	<b>0.05077</b>	<b>0.20758</b>	<b>0.04705</b>	<b>0.19341</b>	

Bold values are obtained from [27]

## References

- [1] RAI AK, GUPTA SS (2021) Nonlinear vibrations of a polar-orthotropic thin circular plate subjected to circularly moving point load. *Composite Structures* 256:112 953.
- [2] Gupta A, Bhardwaj N (2005) Free vibration of polar orthotropic circular plates of quadratically varying thickness resting on elastic foundation. *Applied mathematical modelling* 29(2) 137–157

- [3] LENARTOWICZ A, GUMINIAK M (2020) Free vibrations of iso-and orthotropic plates considering plate variable thickness and interaction with water. *Vibrations in Physical Systems* 31(2)
- [4] CAO Y, ZHONG R, SHAO D, WANG Q, WU D (2019) Free in-plane vibrations of orthotropic rectangular plates by using an accurate solution. *Mathematical Problems in Engineering*
- [5] HACIYEV V, SOFIYEV A, KURUOGLU N (2019) On the free vibration of orthotropic and inhomogeneous with spatial coordinates plates resting on the inhomogeneous viscoelastic foundation. *Mechanics of Advanced Materials and Structures* 26(10) 886–897
- [6] FU Y, YAO J, WAN Z, ZHAO G (2018) Free vibration analysis of moderately thick orthotropic functionally graded plates with general boundary restraints. *Materials* 11(2) 273
- [7] PAPKOV S (2015) Vibrations of a rectangular orthotropic plate with free edges: Analysis and solution of an infinite system. *Acoustical Physics* 61(2) 136–143
- [8] ROUZEGAR J, ABDOLI SHARIFPOOR R (2016) Finite element formulations for free vibration analysis of isotropic and orthotropic plates using two-variable refined plate theory. *SCIENTIA IRANICA* 23(4) 1787–1799
- [9] GUPTA AK, SHARMA S (2014) Free transverse vibration of orthotropic thin trapezoidal plate of parabolically varying thickness subjected to linear temperature distribution. *Shock and Vibration*
- [10] SAYYAD AS, GHUGAL Y (2014) Buckling and free vibration analysis of orthotropic plates by using exponential shear deformation theory. *Latin American Journal of Solids and Structures* 11 1298–1314
- [11] BAHMYARI E, RAHBAR-RANJI A (2012) Free vibration analysis of orthotropic plates with variable thickness resting on non-uniform elastic foundation by element free galerkin method. *Journal of mechanical science and technology* 26(9) 2685–2694
- [12] XING Y, LIU B (2009) New exact solutions for free vibrations of thin orthotropic rectangular plates. *Composite structures* 89(4) 567–574
- [13] ANSARI A (2016) Forced response of polar orthotropic tapered circular plates resting on elastic foundation. *Advances in Acoustics and Vibration*
- [14] XIA X, XU Z, ZHANG Z, HE Y (2017) Bending vibration prediction of orthotropic plate with wave-based method. *Journal of Vibroengineering* 19(3) 1546–1556
- [15] THAI HT, KIM SE (2012) Levy-type solution for free vibration analysis of orthotropic plates based on two variable refined plate theory. *Applied Mathematical Modelling* 36(8) 3870–3882
- [16] ZHANG K, PAN J, LIN TR (2021) Vibration of rectangular plates stiffened by orthogonal beams. *Journal of Sound and Vibration* p 116424

- [17] SHARMA A (2019) Vibration frequencies of a rectangular plate with linear variation in thickness and circular variation in poisson's ratio. *Journal of Theoretical and Applied Mechanics* 57
- [18] BHARDWAJ R, MANI N, SHARMA A (2021) Time period of transverse vibration of skew plate with parabolic temperature variation. *Journal of Vibration and Control* 27(3-4) 323–331
- [19] KHODIYA A, SHARMA A (2021) Temperature effect on frequencies of a tapered triangular plate. *Journal of Applied Mathematics and Computational Mechanics* 20(1) 37–48
- [20] MANI N, KUMAR K, SHARMA A, BHARDWAJ R, KUMAR P (2021) Frequencies of nonuniform triangular plate with two-dimensional parabolic temperature. *In: Soft Computing: Theories and Applications, Springer* 41–51
- [21] LATHER N, SHARMA A (2019) Natural vibration of skew plate on different set of boundary conditions with temperature gradient. *Vibroengineering Procedia* 22 74–80
- [22] SHARMA A, BHARDWAJ R, LATHER N, GHOSH S, MANI N, KUMAR K (2022) Time period of thermal-induced vibration of skew plate with two-dimensional circular thickness *Mathematical Problems in Engineering* 22 p.12
- [23] . LATHER N, BHARDWAJ R, SHARMA A, KUMAR K (2022) Time period analysis of orthotropic skew plate with 2-d circular thickness and 1-d circular density. *Mathematical Problems in Engineering* 22 p.15
- [24] LEISSA AW (1969) Vibration of plates *Scientific and Technical Information Division, National Aeronautics and Space Administration*. 160
- [25] CHAKRAVERTY S (2008) Vibration of plates. *CRC press*
- [26] SHARMA SK, SHARMA AK (2015) Rayleigh-ritz method for analyzing free vibration of orthotropic rectangular plate with 2d thickness and temperature variation. *Journal of Vibroengineering* 17(4) 1989–2000
- [27] SHARMA A, SHARMA AK, RAGHAV A, KUMAR V (2016) Effect of vibration on orthotropic visco-elastic rectangular plate with two dimensional temperature and thickness variation. *Indian Journal of Science and Technology* 9(2) 7